

Compensation technique for the intrinsic error in ultrasound motion estimation using a speckle tracking method

Hirofumi Taki^{1*}, Makoto Yamakawa², Tsuyoshi Shiina³, and Toru Sato⁴

¹Graduate School of Engineering, Tohoku University, Sendai 980-8579, Japan

²Advanced Biomedical Engineering Research Unit, Kyoto University, Kyoto 606-8501, Japan

³Graduate School of Medicine, Kyoto University, Kyoto 606-8501, Japan

⁴Graduate School of Informatics, Kyoto University, Kyoto 606-8501, Japan

E-mail: taki@ecei.tohoku.ac.jp

Received November 27, 2014; accepted March 18, 2015; published online June 8, 2015

High-accuracy ultrasound motion estimation has become an essential technique in blood flow imaging, elastography, and motion imaging of the heart wall. Speckle tracking has been one of the best motion estimators; however, conventional speckle-tracking methods neglect the effect of out-of-plane motion and deformation. Our proposed method assumes that the cross-correlation between a reference signal and a comparison signal depends on the spatio-temporal distance between the two signals. The proposed method uses the decrease in the cross-correlation value in a reference frame to compensate for the intrinsic error caused by out-of-plane motion and deformation without a priori information. The root-mean-square error of the estimated lateral tissue motion velocity calculated by the proposed method ranged from 6.4 to 34% of that using a conventional speckle-tracking method. This study demonstrates the high potential of the proposed method for improving the estimation of tissue motion using an ultrasound speckle-tracking method in medical diagnosis. © 2015 The Japan Society of Applied Physics

1. Introduction

Motion estimation has been employed in several ultrasound techniques such as blood flow imaging,¹⁻⁴ elastic imaging,⁵⁻⁸ phase aberration correction,^{9,10} and assessment of cardiac function.^{8,11-15} Various motion estimation methods based on non-Doppler techniques have been reported; they are primarily classified into two tracking algorithms, speckle tracking and elastic image registration. A speckle tracking method calculates the similarity between the ultrasound data of a reference window in one frame and those of comparison windows in another frame. The shift between the reference window and the best-match comparison window indicates the tissue movement at the reference-window position.¹⁶⁻¹⁹ In contrast, an elastic image registration method deforms a whole image of one frame to adjust that of another frame. After the deformation, the tissue movements at all positions are estimated.^{7,20-24} Both of these methods are considered to be accurate and reliable motion estimators. Heyde et al. have compared these two algorithms for two-dimensional (2D) myocardial motion estimation.²⁵ Additionally, some researchers have reported other motion estimation methods using a 2D measurement plane.^{26,27} However, several studies have reported the differences between the results calculated using the 2D and 3D tissue motion estimators.²⁸⁻³² Previous studies have indicated that the differences might be caused by the intrinsic error involved in the estimation of 3D tissue motion in a 2D measurement plane.^{31,33}

The purpose of the present study is to investigate the intrinsic error involved in estimating 3D tissue motion in a 2D measurement plane using a conventional speckle-tracking method and to propose a compensation method for the error without a priori information. That is, our purpose is to propose a method that compensates for the effect of the out-of-plane (elevation) velocity component on tissue velocity estimation without the measurement of the out-of-plane velocity component. Our previous study investigated a decrease in the cross-correlation as a result of introducing several assumptions in a simulation study under a limited condition.³⁴ In our present study, we demonstrate this

decrease in the estimation accuracy of tissue motion calculated by a speckle tracking method and propose a compensation method that introduces one or two realistic assumptions. Furthermore, we investigate the performance of the proposed compensation method in simulation and experimental studies.

2. Materials and methods

The above decrease in the cross-correlation between a reference window and a comparison window has previously been investigated in studies on atmospheric radar observations.³⁵⁻³⁷ In this section, we first explain the intrinsic error involved in a speckle tracking method that estimates 3D tissue motion in a 2D measurement plane. Next, we verify that the intrinsic error caused by the axial tissue velocity is negligible. We then propose a compensation technique for the intrinsic error involved in using a speckle tracking method caused by out-of-plane motion. We account for the effect of deformation on the cross-correlation. We define the cross-correlation coefficient using ultrasound RF data, which is one of the most established motion estimators. This means that we do not use the envelope cross-correlation. We then describe the simulation and experimental settings.

2.1 Intrinsic error of a speckle tracking method using a 2D measurement plane

Generally, a speckle tracking method defines a reference window in a frame and comparison windows in another frame. The ultrasound data of the reference window is compared with those of comparison windows, and the tissue motion at the reference-window position is estimated from the shift between the reference window and the best-match comparison window.^{38,39} Typically, the ultrasound data in a single scan line are acquired in a transmit event. This means that ultrasound data in a frame are never acquired simultaneously, as emphasized in the current study, because the difference in measurement time between adjacent scan lines in a frame is equal to the pulse-repetition time. Figure 1 shows the effect of out-of-plane motion and deformation on the estimation of tissue motion using a speckle tracking

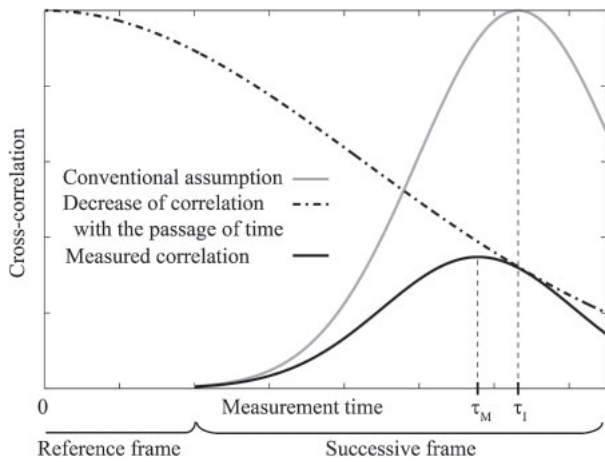


Fig. 1. Forward shift in the measurement time of the best-match comparison window estimated using a speckle tracking method under the condition of out-of-plane tissue motion and deformation, caused by the decrease in the cross-correlation between the ultrasound data of a reference window and that of a comparison window with the passage of time. The measurement time $\tau = 0$ is the acquisition time of a reference signal.

method. The existence of out-of-plane motion and deformation decreases the cross-correlation between the data of a reference window and that of a comparison window with the passage of time. Therefore, a larger decrease occurs at the cross-correlation value in a scan line measured at a later time point. Because the effect of out-of-plane motion and deformation depends on the time passage from the acquisition time of a reference signal, the cross-correlation decreases during the passage of time from the acquisition time of a reference signal (Fig. 1). The conventional speckle-tracking method assumes that the cross-correlation curve has a peak at the measurement time of τ_I , where τ_I is determined by the lateral tissue motion. However, the decrease caused by out-of-plane motion and deformation increases with the passage of time. Therefore, this decrease will cause an unexpected forward shift in the best-match time τ_M from the ideal best-match time τ_I , where τ_I is measured when there is no out-of-plane motion and no deformation. Consequently, the velocity estimated by a speckle tracking method in the beam-scan direction v_{Mx} is smaller than the true tissue velocity in the beam-scan direction v_x .³⁴⁾ It should be noted that $|v_{Mx}| > |v_x|$ when $v_x < 0$.

2.2 Effect of the axial tissue velocity on a speckle tracking method

A conventional speckle-tracking method searches for the best-match comparison window in the measurement plane, as shown in Fig. 2. The conventional method estimates the lateral and axial tissue motion velocities by using the lateral and axial distances (i.e., ξ and ξ_A) between the position of the reference window and that of a comparison window, respectively. This conventional method neglects the effect of the out-of-plane distance because it only accounts for the effects of the lateral and axial distances on the cross-correlation.

The out-of-plane distance between a reference window and a comparison window increases with the passage of time, as shown in Fig. 3. In a case where out-of-plane motion exists, there is no deformation within the window, and when a

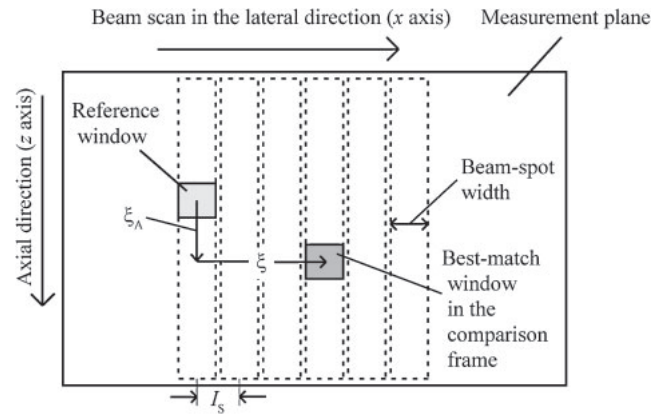


Fig. 2. Schema of a conventional speckle-tracking method using a 2D measurement plane. I_S is the scan line interval. Each broken square denotes the beam of each scan line.

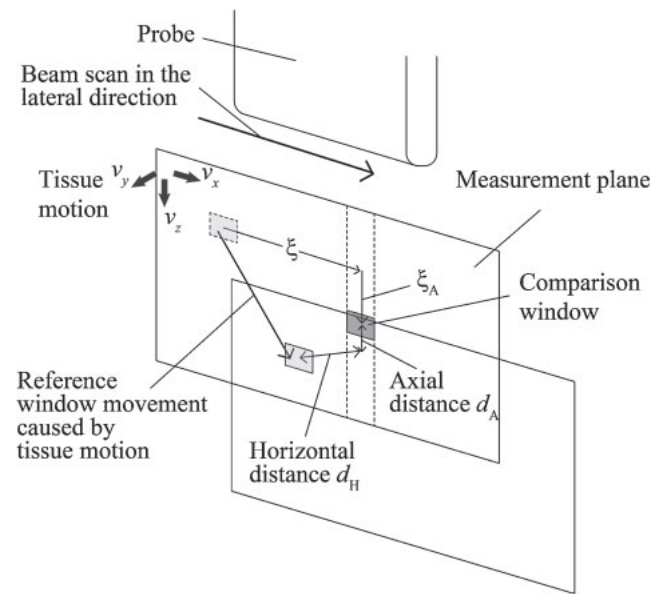


Fig. 3. Schema for the comparison based on a speckle tracking method using a 2D measurement plane. v_x , v_y , and v_z are the lateral, out-of-plane (elevational), and axial tissue velocity components, respectively.

circular ultrasound beam spot is employed, the expectation of a cross-correlation value should depend on two parameters: the axial distance d_A and horizontal distance d_H between the position of the reference window on the tissue at the comparison time and the position of the comparison window. In the present study, we define the beam spot in a measurement range as the region where the echo intensity from a point scatterer in the region is larger than 25% of the peak echo intensity from a point scatterer. The horizontal distance is the distance perpendicular to the axial direction, as shown in Fig. 3. The axial and horizontal distances are expressed by Eqs. (1) and (2), respectively, as follows:

$$d_A = |v_z\tau - \xi_A| = \left| \left(\frac{c}{2} - v_z \right) \tau - \frac{n_T c T_{PR}}{2} \right|, \quad (1)$$

$$d_H = \sqrt{(v_x\tau - \xi)^2 + (v_y\tau)^2}, \quad (2)$$

where τ is the measurement time of a comparison window, c is the sound velocity, T_{PR} is the pulse repetition time, the signal of the comparison window is acquired in the $(n_T + 1)$ th

transmit event, and v_x , v_y , and v_z are the lateral, out-of-plane (elevational) and axial tissue velocity components, respectively. A reference window is measured at $\tau = 0$ in the first transmit event, and the lateral position of the reference window is $\xi = 0$. The conventional method neglects the term $(v_y\tau)^2$ in Eq. (2). We introduce an assumption that the cross-correlation depends on the spatial distance d_{AH} , which satisfies the following equation:

$$d_{AH}^2 = \alpha d_A^2 + d_H^2, \quad (3)$$

where α is a positive value. The effect of the axial distance on the cross-correlation may depend on half the pulse width and that of the horizontal distance may depend on the beam-spot width. Because the beam-spot width is larger than half the pulse width in most cases, α may be larger than 1. When ξ is a constant (i.e., in each scan line), d_{AH} is minimized at $\tau = \tau_{\min}$ and τ_{\min} is expressed by

$$\tau_{\min} = \frac{v_x\xi + \alpha\left(\frac{c}{2} - v_z\right)\frac{n_TcT_{PR}}{2}}{v_x^2 + v_y^2 + \alpha\left(\frac{c}{2} - v_z\right)^2} \cong \frac{n_TcT_{PR}}{c - 2v_z}, \quad (4)$$

because typically $|c/2 - v_z| \gg |v_x|, |v_y|$ and $n_TcT_{PR} \gg \xi$. Equation (4) indicates that d_A should be 0 when d_{AH} is minimized subject to a constant ξ . That is, the axial position of the best-match comparison window in each scan line should be the same as that of the reference window at the comparison time. Therefore, the cross-correlation depends on the horizontal distance d_H when the cross-correlation value of the axial-best-match position in each scan line is used.

The approximation in Eq. (4) is valid because the variation in the measurement time in the axial direction is much smaller than that in the lateral direction. The difference in the measurement time between two adjacent scan lines with the same depth is equal to the pulse-repetition time T_{PR} . When $T_{PR} = 0.12$ ms and the scan line interval is 0.36 mm, the variation in the measurement time in the lateral direction is 0.33 ms/mm. In contrast, the variation in the measurement time in the axial direction is 1.33 μ s/mm because it is determined by the sound velocity c . When the tissue velocity is less than 2 m/s, the tissue movement caused by a time passage of 1.33 μ s is less than 2 μ m. Therefore, the variation in the measurement time in the axial direction is much smaller than that in the lateral direction, indicating the validity of the approximation in Eq. (4). Consequently, the unexpected position shift of the best-match comparison window caused by the axial tissue movement is negligible.

2.3 Compensation method for the intrinsic error involved in a conventional speckle-tracking method in a case with out-of-plane motion

First, we describe the proposed compensation method in the case of using a circular ultrasound beam, that is, the lateral beam width is equal to the elevational beam width. We then expand the proposed method to the case of using an elliptical ultrasound beam spot, that is, the lateral beam width is different from the elevational beam width. In this study, we assume that ultrasound beams of all scan lines have the same beam-spot shape.

Equation (4) indicates that the axial position of the best-match comparison window in a scan line should be the same

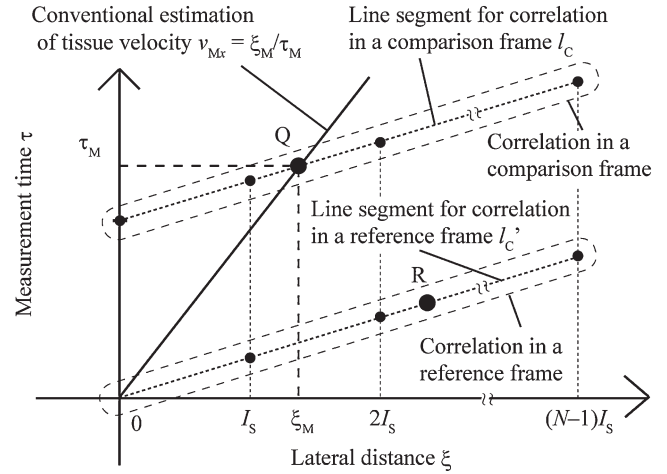


Fig. 4. Locations of cross-correlation values in the ξ - τ plane, where the values are acquired in a single measurement plane. ξ and τ are the distance in the x direction and the difference in measurement time between a reference window and a comparison window, respectively. Small dots denote measured axial-best-match cross-correlation values. Point Q is the best-match position in a comparison frame. Point R exists in a reference frame, where it has the same correlation value as Q.

as that of the reference-window position at the comparison time, namely $d_A = 0$. Therefore, this is the key point of the proposed method; we introduce a simple and realistic assumption that the axial-best-match cross-correlation value depends on the horizontal distance between the position of the reference window at the comparison time and that of the comparison window d_H . First, the proposed method selects the best-match position in the line segment of a comparison frame, point Q, as shown in Fig. 4. The line segment of a comparison frame l_c is determined by the lateral distance ξ and measurement time τ at the peak cross-correlation position along each scan line (ξ and τ at the axial best-match positions) in a comparison window. Most conventional speckle-tracking algorithms estimate the lateral tissue motion by using the position of Q. Next, the proposed method searches for the position of point R in a reference frame, where R has the same correlation value as Q. Because the cross-correlation value at a point on the line l'_c decreases monotonically as the distance between the origin and the point increases, we can determine point R using interpolation or extrapolation. The axial-best-match cross-correlation value should decrease with the increase in the horizontal distance d_H , and thus a contour of the cross-correlation value describes an ellipse in the ξ - τ plane. The concept of the “cross-correlation contour” is the same as the concept of contour lines on a map, where the cross-correlation coefficients are identical on each contour. Because points Q and R have the same correlation coefficients, there is an ellipse contour that passes through them, as shown by the solid curve in Fig. 5. Q represents the peak value of the cross-correlation in a comparison frame. Therefore, the ellipse contour must be tangential to the line segment of the comparison frame l_c at Q because the intersection of the ellipse and l_c at Q means that Q does not have the peak cross-correlation value on l_c . We can determine the ellipse contour by using the two pieces of information: it passes through R and it is tangential to l_c at Q. The proposed method estimates the lateral tissue motion by using the ellipse contour. As shown in Figs. 4 and 5, no

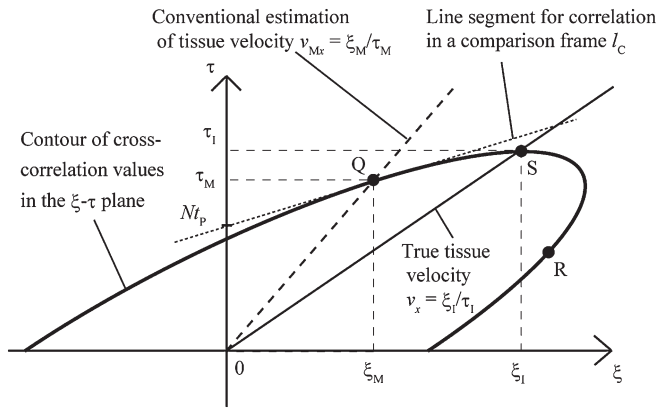


Fig. 5. Axial-best-match cross-correlation map in the ξ - τ plane. ξ and τ are the distance in the x direction and the difference in measurement time between a reference window and a comparison window, respectively. ξ_M and τ_M are the measured distance and time difference using a conventional speckle-tracking method, respectively. ξ_1 and τ_1 are the measured distance and time difference using the proposed compensation technique, respectively.

a priori information is required regarding the tissue motion for the proposed compensation method.

The cross-correlation value on an ellipse contour is constant, and thus the horizontal distance d_H is also constant on a contour. Because the derivative of Eq. (2) with respect to ξ becomes $v_x\tau - \xi = 0$, the maximal point of an ellipse contour, point S in Fig. 5, is located on the line $v_x\tau - \xi = 0$. Therefore, the proposed compensation technique estimates the lateral tissue motion velocity v_x by localizing the position of S, where the localization of S requires only the derivative of the acquired function of the ellipse contour with respect to ξ . This compensation method is termed full correlation compensation (FCC). The gap between points Q and S should be the intrinsic error in motion estimation in the lateral direction based on a speckle tracking method using a 2D measurement plane.

When an elliptical ultrasound beam spot is employed, Eq. (2) is modified to

$$d_E = \sqrt{(v_x\tau - \xi)^2 + (B_R v_y \tau)^2}, \quad (5)$$

where B_R is the ratio of the beam-spot size in the x direction to that in the y direction. This equation is based on the modified assumption that the axial-best-match cross-correlation value depends on the square measure of the overlap between the beam spot of the reference window at the comparison time and that of the comparison window. Equation (5) indicates that a contour of the cross-correlation value also depicts an ellipse in the ξ - τ plane. Its maximal point of τ in terms of ξ also indicates the true velocity v_x because the derivative of Eq. (5) with respect to ξ also becomes $v_x\tau - \xi = 0$. Therefore, in the case where an elliptical ultrasound beam spot is employed, the proposed compensation method can be used with no additional modification.

2.4 Compensation method for the intrinsic error involved in a speckle tracking method in the case with both out-of-plane motion and deformation

When tissue deformation occurs, the axial-best-match cross-correlation value should depend on two parameters: one is the difference in measurement time between a reference

window and the comparison window τ and the other is the horizontal distance d_H . The conventional speckle-tracking methods neglect the former parameter and the horizontal distance in the y direction.

In this case, we introduce an additional assumption that the axial-best-match cross-correlation value depends on the spatio-temporal distance given by the following equation:

$$d'_H = \sqrt{d_H^2 + \beta\tau^2}, \quad (6)$$

where β is a positive number. When an elliptical ultrasound beam is employed, a contour of the cross-correlation value depicts the ellipse given by

$$(v_x\tau - \xi)^2 + (B_R^2 v_y^2 + \beta)\tau^2 = D, \quad (7)$$

where $D = d_H'^2$ is a positive constant. Equation (7) indicates that a contour of the cross-correlation value also depicts an ellipse in the ξ - τ plane, where its maximal point of τ in terms of ξ also indicates the true velocity v_x . Therefore, the proposed compensation method can be used with no additional modification.

2.5 Estimation of tissue motion using cross-correlation coefficients

The cross-correlation coefficient is one of the most established motion estimators.^{38,39)} Therefore, we refer to the motion estimator using the cross-correlation coefficients as the conventional speckle-tracking method. In this study, we applied the proposed compensation technique, FCC, to a speckle tracking method using the cross-correlation coefficient in simulation and experimental studies. The cross-correlation coefficient between two successive frames at the axial-best-match comparison window is defined as follows:

$$C_C(x_R, z_R, \xi) = \max_u \frac{\sum_{z=z_R-W_z/2}^{z_R+W_z/2} f(x_R, z)g(x_R + \xi, z + u)}{\sqrt{\sum_{z=z_R-W_z/2}^{z_R+W_z/2} f^2(x_R, z) \sum_{z=z_R-W_z/2}^{z_R+W_z/2} g^2(x_R + \xi, z + u)}}, \quad (8)$$

where x_R and z_R are the x and z coordinates of the reference-window position, u is the search range in the axial direction, i.e., in the z direction, W_z is the window size in the axial direction, and $f(x, z)$ and $g(x, z)$ are the ultrasound RF data of the reference and comparison frames, respectively. The cross-correlation coefficient between scan lines in the reference frame at the axial-best-match comparison window is defined as follows:

$$C_R(x_R, z_R, \xi) = \max_u \frac{\sum_{z=z_R-W_z/2}^{z_R+W_z/2} f(x_R, z)f(x_R + \xi, z + u)}{\sqrt{\sum_{z=z_R-W_z/2}^{z_R+W_z/2} f^2(x_R, z) \sum_{z=z_R-W_z/2}^{z_R+W_z/2} f^2(x_R + \xi, z + u)}}. \quad (9)$$

2.6 Simulation setup

We investigated the performance of the proposed compensation method in a simulation study based on a 3D ray-tracing algorithm. In the simulation study, we assumed that the

position of the k th scatterer in the tissue at the n th transmit event can be expressed by the following equations:

$$\mathbf{P}_{S_k}(\tau) = \mathbf{P}_{S_k}(0) + \tau(\mathbf{v} + \mathbf{v}_{Rk}), \quad (10)$$

$$\tau = (n - 1)T_{PR}, \quad (11)$$

where \mathbf{v} and \mathbf{v}_{Rk} are the translational components of the tissue motion velocity and random motion velocity, respectively. We investigated the performance of the proposed method under the conditions of $-1 \leq v_x \leq 1$ m/s, $0 \leq v_y \leq 1.5$ m/s, and $v_z = 0$ m/s, where v_x , v_y , and v_z are the x , y , and z components of \mathbf{v} , respectively. In this setting, the out-of-plane motion was simulated by v_y . The norm of the random motion \mathbf{v}_{Rk} follows a Gaussian distribution, where the direction of \mathbf{v}_{Rk} is random (i.e., its z component is not zero), v_y is the out-of-plane motion, and \mathbf{v}_{Rk} causes deformation. In the case with deformation, we assumed that the norm of the random motion velocity follows a Gaussian distribution with an average value of zero and a standard deviation of 0.05 m/s.

We calculated the ultrasound data at the n th transmit event, i.e., at the measurement time of τ , using the following formulae:

$$f_n(z) = \sum_k 2^{-d_H^2} s(z - |\mathbf{P}_{S_k}(\tau) - (x_n, 0, 0)|), \quad (12)$$

$$d_H = \sqrt{\left(\frac{p_{S_{kx}}(\tau) - x_n}{B_x}\right)^2 + \left(\frac{p_{S_{ky}}(\tau)}{B_y}\right)^2}, \quad (13)$$

where the center frequency of $s(z)$ in the time domain is 5 MHz and its -3 dB fractional bandwidth is 60%, the sound velocity c is 1500 m/s, and the sampling frequency is 30 MHz. x_n is the x coordinate of the scan line at the n th transmit event, $p_{S_{kx}}(\tau)$ and $p_{S_{ky}}(\tau)$ are the x and y coordinates of the position vector $\mathbf{P}_{S_k}(\tau)$, and B_x and B_y are the -6 dB beam-spot widths in the x and y directions, respectively. The center of the tissue with scatterers was situated at a depth of 40 mm. The tissue size was 30, 20, and 15 mm in the x , y , and z directions, respectively. Scatterers were distributed randomly in the tissue and their density was five scatterers per cube of the wavelength at the center frequency, as originally described in a previous study.⁴⁰⁾ Therefore, a total of 1.67×10^6 scatterers was used. We employed a 2D spatial median filter with a kernel size of 3×3 in the tissue velocity estimation, which has been commonly used to eliminate outliers.^{26,41)} The grid size of the measurement region was 1.08 and 1.0 mm in the x and y directions, respectively. Consequently, by using the 2D spatial median filter, each sample was selected from nine estimated velocities in the region size of 3.24 and 3.0 mm in the x and y directions, respectively. This size is sufficiently larger than the speckle size.

To suppress the contribution of out-of-plane motion and deformation, the difference in measurement time between the reference window and a comparison window should be shortened. We thus employed the setting that each frame consists of three scan lines and the successive frame of the reference frame was used for the comparison frame. We acquired the ultrasound data of five frames to calculate the expectation of the cross-correlation coefficient. The pulse-repetition time T_{PR} was 0.12 ms and the window size in the axial direction W_z was 1.0 mm. The scan line interval I_S was

0.36 mm. The search range u ranged from -1 to 1 mm. When the pulse-repetition time T_{PR} is 0.12 ms and the tissue movement in the lateral direction v_x is 1.0 m/s, a typical speckle-tracking method requires a scan line interval I_S of larger than 0.24 mm to catch up with the reference window in the successive comparison frame. Because the scan line interval of the data acquired by a commercial diagnostic ultrasound (US) device was 0.12 mm, we defined the scan line interval I_S as 0.36 mm, which is three times the scan line interval acquired by the commercial US device used in the experimental study.

2.7 Experimental setup

Experiments were conducted using a Hitachi EUB-8500 US device with a 5 MHz linear array to acquire raw in-phase and quadrature (IQ) data. The scan line interval in the x direction was 0.12 mm. IQ data were converted to radio frequency (RF) data using the RF data oversampling technique.⁴²⁾ The ultrasound beam-spot width at a depth of 40 mm was 0.6 and 1.9 mm in the x and y directions, respectively. We prepared a Model 049 elasticity phantom (Computerized Imaging Reference Systems). In the experimental study, we also employed a setting where each frame consists of three scan lines and the successive frame of the reference frame was used for the comparison frame. The parallel movement of the probe in the elevational direction simulated the tissue movement in the elevational direction. The tissue movement in the lateral direction was simulated by the selection of suitable scan lines. Because the setting intervals of the tissue motion velocity in the x and y directions were 0.5 and 0.25 m/s, the x and y components of the tissue motion in a pulse-repetition time were multiples of 0.06 and 0.03 mm, respectively. We thus acquired the ultrasound data of several measurement planes, where the measurement plane interval in the y direction was 0.03 mm. Because the scan line interval of the linear array probe was 0.12 mm, we constructed the ultrasound data with a 0.06 mm scan line interval in the x direction using linear interpolation. The locations of the selected scan lines were calculated from the location of the scan line after the compensation for the tissue movement at the measurement time. In the experimental study, we also used a 2D spatial median filter with a kernel size of 3×3 . We used 10 samples to investigate the performance of the conventional method and the FCC technique, with the exception of the 2D-image study.

3. Results

3.1 Investigation of the FCC technique in a simulation study with out-of-plane motion

Figure 6 shows the tissue motion velocity in the beam-scan direction at a depth of 4 cm estimated using a conventional speckle-tracking method and the FCC technique in a simulation study based on a 3D ray-tracing algorithm. No random motion existed and the ultrasound beam-spot width was 0.6 and 1.9 mm in the x and y directions, respectively. Each average value was calculated using 10 samples. The tissue motion velocity estimated using the conventional speckle-tracking method decreased as the velocity of out-of-plane motion increased. This result is consistent with the method described in Sect. 2.1. The root-mean-square errors (RMSEs) of the averaged velocities estimated using the

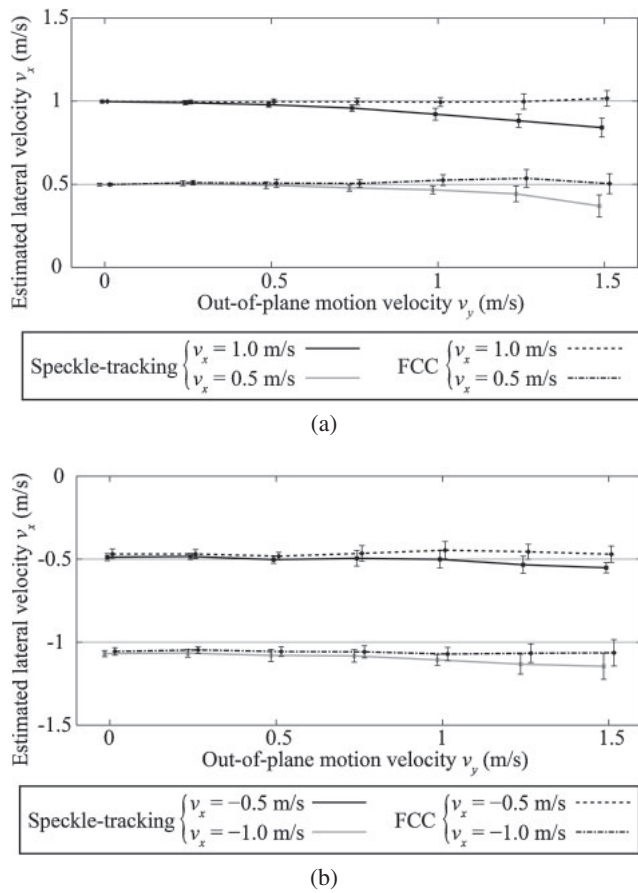


Fig. 6. Tissue motion velocity in the beam-scan direction at a depth of 4 cm estimated using the conventional speckle-tracking method and the proposed FCC compensation technique in the simulation study, where the tissue velocity in the z direction is 0 m/s. The true velocities in the x direction are (a) 1.0 and 0.5 m/s and (b) -0.5 and -1.0 m/s. Ten samples are averaged. The tissue motion in the y direction, i.e., the out-of-plane motion, ranges from 0 to 1.5 m/s and no deformation occurs. The ultrasound beam-spot width is 0.6 and 1.9 mm in the x and y directions, respectively.

conventional speckle-tracking method were 0.082 and 0.056 m/s when the x components of the tissue motion velocity v_x were 1.0 and 0.5 m/s, respectively. The y components of the tissue motion velocity, namely the velocity of out-of-plane motion, ranged from 0 to 1.5 m/s. We calculated the RMSE v_{ERR} by the following formula:

$$v_{ERR} = \sqrt{\frac{1}{N_y} \sum_{v_y=0}^{v_{yM}} |v_{Ex}(v_y) - v_{Tx}|^2}, \quad (14)$$

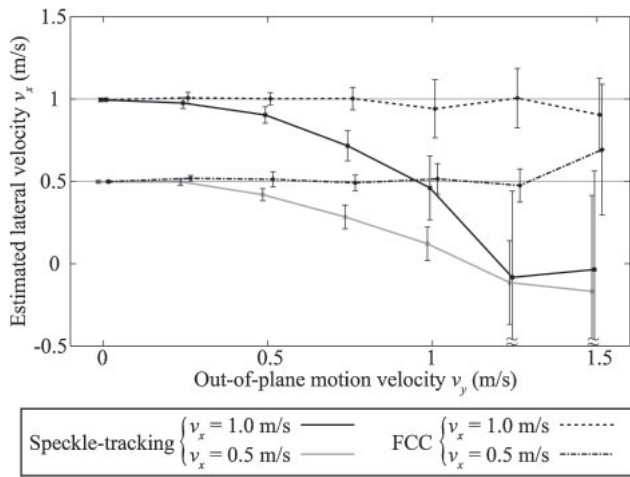
where N_y is the number of variations in the out-of-plane motion velocity v_y , v_{yM} is the maximum value of v_y , $v_{Ex}(v_y)$ is the average estimated lateral velocity after 2D spatial median filtering at the out-of-plane motion of v_y , and v_{Tx} is the true lateral velocity. The RMSE indicates the estimation error of the lateral tissue velocity compared with the true lateral velocity.

The RMSEs using the FCC technique were 0.007 and 0.017 m/s when $v_x = 1.0$ and 0.5 m/s, respectively. The averages of all the tissue velocities in the range of $0 \leq v_y \leq 1.5$ m/s estimated using the speckle tracking algorithm were 0.939 (0.030) and 0.465 (0.033) m/s when $v_x = 1.0$ and 0.5 m/s, respectively. Standard deviations are given in parentheses. Because 10 samples existed in each out-of-plane

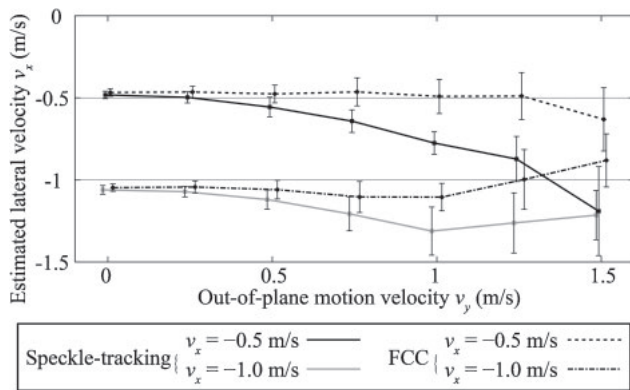
motion, 70 samples were used for the stochastic investigation. In contrast, the averages using the FCC technique were 1.000 (0.028) and 0.512 (0.034) m/s. In both cases of $v_x = 1.0$ and 0.5 m/s, the estimated velocities using the conventional method and the FCC technique are statistically significant ($P < 10^{-10}$; Student's t -test). When $v_x = 1.0$ and 0.5 m/s, in the range of $0 \leq v_y \leq 1.5$ m/s, the employment of the FCC technique suppressed the RMSE of the estimated velocity to 8.7 and 30%, respectively, of that using the conventional speckle-tracking method. The FCC technique also succeeded in preventing overestimation of the tissue motion velocity when no out-of-plane velocity existed, i.e., $v_y = 0$ m/s. In addition, the FCC technique compensated for the large effect of the out-of-plane velocity at $v_y = 1.5$ m/s, and it suppressed the estimation error at $(v_x, v_y) = (1.0 \text{ m/s}, 1.5 \text{ m/s})$ and $(0.5 \text{ m/s}, 1.5 \text{ m/s})$ to 11 and 2.6%, respectively, of that using the conventional speckle-tracking method.

The poor performance of the conventional speckle-tracking method and the FCC technique in the case of $v_x < 0$ m/s was caused by the wide beam-spot interval on the tissue. Because the scan line interval was set to 0.36 mm and the pulse-repetition time was set to 0.12 ms in the current study, the tissue moved by -0.06 mm in the beam-scan direction at $v_x = -0.5$ m/s during a single pulse-repetition time. Therefore, the beam-spot intervals on the tissue in the x direction were 0.24, 0.30, 0.42, and 0.48 mm at $v_x = 1.0, 0.5, -0.5,$ and -1.0 m/s, respectively. Because we employed a beam-spot width of 0.6 mm, a beam-spot interval of 0.42 mm or wider should suppress the accuracy in calculating the peak cross-correlation coefficient at the successive frame. The FCC technique uses the peak value of the cross-correlation coefficient in the successive frame to compensate for the error in the estimation of motion, and thus the low accuracy in calculating the peak value decreases the performance of the FCC technique.

Figure 7 shows the estimated velocity in the beam-scan direction when no random motion existed and the ultrasound beam-spot width was 0.6 mm in both the x and y directions. The conventional speckle-tracking method used in the current study considerably underestimated the velocity in the beam-scan direction as the out-of-plane motion increased, as compared with the results obtained using the beam-spot sizes of 0.6 and 1.9 mm in the x and y directions (Fig. 6). The large underestimation of velocity should be caused by the narrow beam-spot width in the y direction, which emphasizes the effect of out-of-plane motion on the estimation of the velocity in the beam-scan direction, as shown in Eq. (5). When the y component of the tissue motion velocity ranged from 0 to 1.0 m/s, the RMSEs of the averaged velocities estimated using the conventional speckle-tracking method were 0.276, 0.198, 0.141, and 0.181 m/s when the true tissue motion velocity in the beam-scan direction was 1.0, 0.5, -0.5, and -1.0 m/s, respectively. In contrast, the RMSEs using the FCC technique were 0.027, 0.013, 0.029, and 0.077 m/s. The averages of all the tissue velocities in the range of $0 \leq v_y \leq 1.0$ m/s estimated using the speckle tracking method were 0.810 (0.095), 0.364 (0.057), -0.590 (0.052), and -1.154 (0.083) m/s when $v_x = 1.0, 0.5, -0.5,$ and -1.0 m/s, respectively. In contrast, the averages using the FCC technique were 0.990 (0.084), 0.507 (0.050), -0.472



(a)



(b)

Fig. 7. Tissue motion velocity in the beam-scan direction at a depth of 4 cm estimated using the conventional speckle-tracking method and the FCC technique in the simulation study, where the tissue velocity in the z direction is 0 m/s. The true velocities in the x direction are (a) 1.0 and 0.5 m/s and (b) -0.5 and -1.0 m/s. The tissue motion velocity in the y direction ranges from 0 to 1.5 m/s and no deformation occurs. The ultrasound beam-spot width is 0.6 mm in both the x and y directions.

(0.065), and -1.072 (0.062) m/s. In all cases, the estimated velocities obtained using the conventional method and the FCC technique were statistically significant ($P < 10^{-7}$). When $v_x = 1.0$ and 0.5 m/s, the employment of the FCC technique not only suppressed the RMSE of the estimated velocity to 9.7 and 6.4%, respectively, of that calculated using the conventional method, but also decreased the standard deviation of the estimated velocity. This result indicates that the employment of a narrow slice thickness causes a large estimation error using the conventional speckle-tracking method and that the FCC technique effectively compensates for the large estimation error.

When $v_x = -0.5$ and -1.0 m/s, the beam-spot intervals on the tissue were 0.42 and 0.48 mm, respectively. The wide beam-spot intervals caused the decrease in the performance of both the speckle tracking method and the FCC technique, as shown in Fig. 6(b). However, in the case of using the 0.6 mm beam spot, the FCC technique succeeded in suppressing the RMSE of the estimated velocity to less than half of that using the conventional speckle-tracking method, as shown in Fig. 7(b). The improvement using the FCC technique might have originated from the large underestimation of the tissue velocity using the speckle tracking

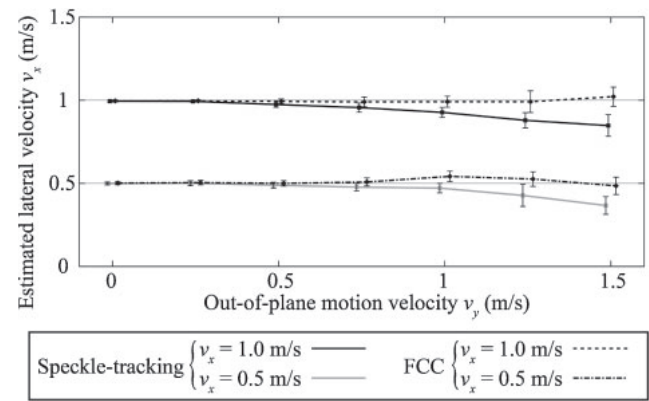


Fig. 8. Tissue motion velocity in the beam-scan direction at a depth of 4 cm estimated using the conventional speckle-tracking method and the FCC technique in the simulation study, where the tissue velocity in the z direction is 0.5 m/s. The true velocities in the x direction are 1.0 and 0.5 m/s. The tissue motion velocity in the y direction ranges from 0 to 1.5 m/s and no deformation occurs. The ultrasound beam-spot width is 0.6 and 1.9 mm in the x and y directions, respectively.

method. This result indicates that when out-of-plane motion causes a large estimation error, the FCC technique may suppress the error even under the severe condition that the beam-spot interval on the tissue is wider than half of the beam-spot width.

Figure 8 shows the tissue motion velocity in the beam-scan direction at a depth of 4 cm estimated using the conventional speckle-tracking method and the FCC technique, where the tissue velocity in the z direction, v_z , is 0.5 m/s. No random motion existed and the ultrasound beam-spot width was 0.6 and 1.9 mm in the x and y directions, respectively. The tissue motion velocity shown in Fig. 8 is very close to that when the tissue velocity in the z direction is 0 m/s shown in Fig. 6(a). In both cases using the conventional method and the FCC technique, the estimated lateral velocities in the cases of $v_z = 0$ and 0.5 m/s are statistically insignificant ($P > 0.25$). This result indicates the validity of our supposition that the cross-correlation depends on the horizontal distance d_H . This result supports the finding that the estimation error of the lateral tissue velocity caused by the axial tissue movement is negligible.

3.2 Investigation of the FCC technique in a simulation study with both out-of-plane motion and deformation

Figure 9 shows the estimated tissue motion velocity in the beam-scan direction at a depth of 4 cm, where random motion existed and the ultrasound beam-spot width was 0.6 and 1.9 mm in the x and y directions, respectively. Each average velocity was calculated using 10 samples. The RMSEs of the averaged velocities estimated using the conventional speckle-tracking method were 0.159, 0.119, 0.077, and 0.150 m/s when $v_x = 1.0, 0.5, -0.5,$ and -1.0 m/s, respectively. The y components of the tissue motion velocity ranged from 0 to 1.5 m/s. In contrast, the RMSEs of the averaged velocities estimated using the FCC technique were 0.016, 0.013, 0.032, and 0.078 m/s. The averages of the tissue velocities in the range of $0 \leq v_y \leq 1.5$ m/s estimated using the speckle tracking method were 0.851 (0.057), 0.389 (0.049), -0.564 (0.054), and -1.146 (0.055) m/s when $v_x = 1.0, 0.5, -0.5,$ and -1.0 m/s, respectively. In contrast, the averages using

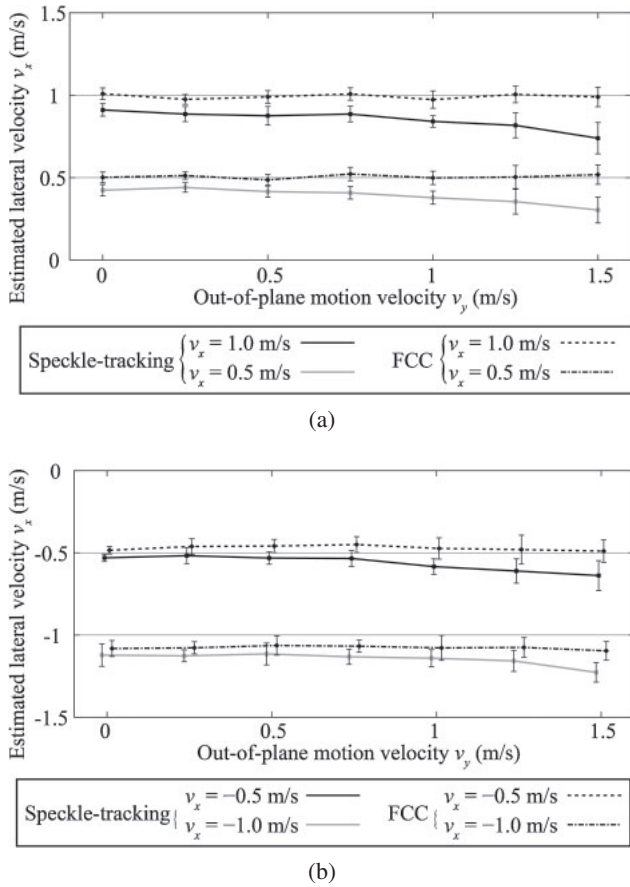


Fig. 9. Tissue motion velocity in the beam-scan direction at a depth of 4 cm estimated using the conventional speckle-tracking method and the FCC technique in the simulation study. The true velocities in the x direction are (a) 1.0 and 0.5 m/s and (b) -0.5 and -1.0 m/s. The tissue motion in the y direction ranges from 0 to 1.5 m/s and deformation caused by random motion exists. The ultrasound beam-spot width is 0.6 and 1.9 mm in the x and y directions, respectively.

the FCC technique were 0.993 (0.042), 0.506 (0.043), -0.471 (0.055), and -1.077 (0.053) m/s. In all cases, the estimated velocities using the conventional method and the FCC technique are statistically significant ($P < 10^{-10}$).

When $v_x = 1.0, 0.5, -0.5,$ and -1.0 m/s, in the range of $0 \leq v_y \leq 1.5$ m/s the employment of the FCC technique suppressed the RMSE of the estimated velocity to 9.8, 11, 42, and 52%, respectively, of that calculated using the conventional speckle-tracking method. This result indicates that the existence of deformation will suppress the performance of the FCC technique; however, the employment of the FCC technique is beneficial to compensate for the underestimation of the conventional speckle-tracking method caused by out-of-plane motion and deformation.

3.3 Investigation of the FCC technique in an experimental study

Figure 10 shows the tissue motion velocity in the beam-scan direction at a depth of 4 cm estimated by the conventional speckle-tracking method and the FCC technique in an experimental study. In this study, we used an elasticity phantom. No random motion existed and the ultrasound beam-spot width at a depth of 4 cm was 0.6 and 1.9 mm in the x and y directions, respectively. Each average velocity was calculated using 10 samples.

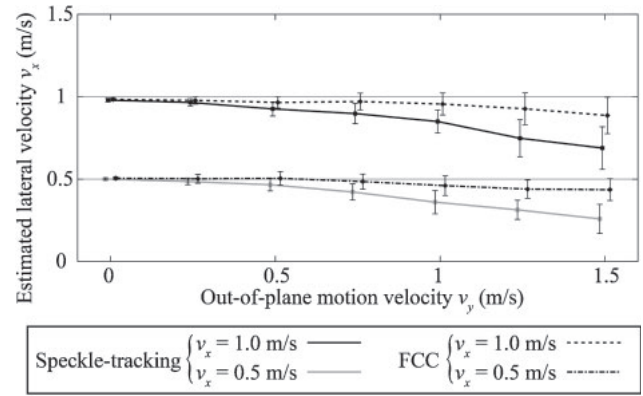


Fig. 10. Tissue motion velocity in the beam-scan direction at a depth of 4 cm estimated by the conventional speckle-tracking method and the FCC technique in the experimental study using an elasticity phantom. The true velocities in the beam-scan direction are 1.0 and 0.5 m/s. The tissue motion in the y direction ranges from 0 to 1.5 m/s and no deformation occurs. The ultrasound beam-spot width at the depth of 4 cm is 0.6 and 1.9 mm in the x and y directions, respectively.

In the study using an elasticity phantom with scatterers, the RMSEs of the averaged velocities estimated using the conventional speckle-tracking method were 0.169 and 0.131 m/s when $v_x = 1.0$ and 0.5 m/s, respectively. The y components of the tissue motion velocity ranged from 0 to 1.5 m/s. In contrast, the RMSEs using the FCC technique were 0.057 and 0.037 m/s. The averages of the tissue velocities in the range of $0 \leq v_y \leq 1.5$ m/s estimated using the conventional method were 0.865 (0.073) and 0.401 (0.052) m/s when $v_x = 1.0$ and 0.5 m/s, respectively. In contrast, the averages using the FCC technique were 0.952 (0.063) and 0.476 (0.045) m/s. When $v_x = 1.0$ and 0.5 m/s, in the range of $0 \leq v_y \leq 1.5$ m/s the employment of the FCC technique not only suppressed the RMSE of the estimated velocity to 34 and 28%, respectively, of that calculated using the conventional speckle-tracking method but also decreased the standard deviation of the estimated velocity.

Figure 11 shows the tissue motion velocity and its error in the beam-scan direction in a 2D measurement plane estimated using the conventional speckle-tracking method and the FCC technique in an experimental study using an elasticity phantom, where the true velocity in the x direction v_x was 0.5 m/s. The tissue motion velocity in the y direction v_y was 0, 0.25, and 0.5 m/s in the ranges of $x < -3.24$ mm, $-3.24 \leq x \leq 3.24$ mm, and $3.24 \text{ mm} < x$, respectively. The grid size of the measurement region was 1.08 and 1.0 mm in the x and y directions, respectively. We also employed the 2D spatial median filter with a kernel size of 3×3 .

We investigated the error of the proposed method in estimating the tissue motion velocity in the x direction using the RMSE. The RMSEs of the estimated velocities using the conventional speckle-tracking method were 0.006, 0.018, and 0.052 m/s when $v_y = 0, 0.25,$ and 0.5 m/s, respectively. Sixty samples were used for the stochastic investigation in each case for v_y . In contrast, the RMSEs using the FCC technique were 0.009, 0.012, and 0.042 m/s. The averages of the tissue velocities estimated using the speckle tracking algorithm were 0.500 (0.006), 0.488 (0.014), and 0.470 (0.042) m/s when $v_y = 0, 0.25,$ and 0.5 m/s, respectively. In contrast, the averages using the FCC technique were 0.507 (0.006), 0.499

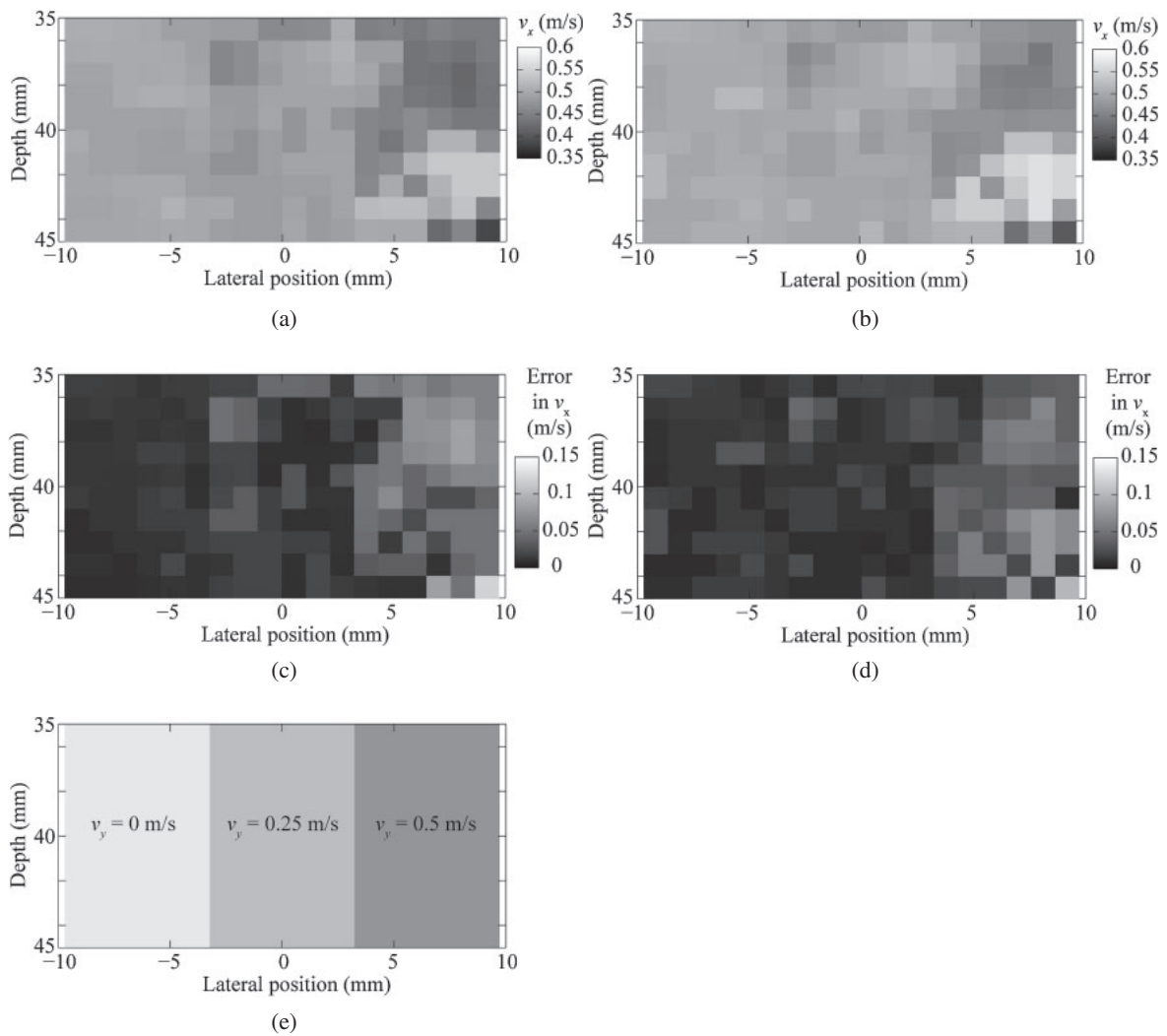


Fig. 11. Estimated tissue motion velocity in the x direction v_x , i.e., in the beam-scan direction, in a 2D measurement plane (a) using the conventional speckle-tracking algorithm and (b) using the FCC technique in the experimental study, where an elasticity phantom is used. The true tissue velocity in the beam-scan direction v_x is 0.5 m/s. Error in estimated tissue motion velocity in the x direction v_x (c) using the conventional speckle-tracking algorithm and (d) using the FCC technique in the experimental study. (e) In this setting, the tissue motion in the y direction v_y , i.e., the out-of-plane motion, is 0, 0.25, and 0.5 m/s in the ranges of $x < -3.24$ mm, $-3.24 \leq x \leq 3.24$ mm, and $3.24 < x$, respectively. The grid size of the measurement region is 1.08 and 1 mm in the x and y directions, respectively. The ultrasound beam-spot size at a depth of 4 cm is 0.6 and 1.9 mm in the x and y directions, respectively.

(0.012), and 0.494 (0.042) m/s. In all cases, the estimated velocities using the conventional method and the FCC technique were statistically significant ($P < 0.002$). The conventional speckle-tracking method increasingly underestimated the lateral tissue motion velocity v_x as the out-of-plane motion v_y progressively increased. In contrast, the FCC technique succeeded in estimating the lateral tissue motion velocity with an error of less than 0.007 m/s. This result supports the view that the FCC technique improves the performance of an ultrasound cross-correlation technique in medical diagnosis, for example, in the assessment of cardiac function.

4. Discussion

As described in Sect. 3.1, the beam-spot interval on the tissue becomes narrow when the lateral tissue velocity v_x has a large positive value. Because a narrow beam-spot interval on the tissue results in high accuracy in interpolating cross-correlation values, when $v_x = 1.0$ m/s, the accuracy in interpolating the cross-correlation value becomes the greatest. This is the most probable reason why the FCC technique

has a high performance when v_x is positive, as shown in Figs. 6(a), 7(a), and 9(a). When v_x is negative, i.e., Figs. 6(b), 7(b), and 9(b), the time difference between a reference window and the best-match comparison window is smaller than that when v_x is positive, because the tissue movement at $v_x < 0$ m/s is opposite to the beam scan direction. Therefore, the error in the cross-correlation caused by the out-of-plane motion and deformation should be small when v_x is negative, resulting in the high performance of the conventional speckle-tracking method at $v_x < 0$ m/s, as shown in Figs. 6(b), 7(b), and 9(b).

When $v_x = 1.0$ m/s, the existence of deformation suppressed the performance of the FCC technique, as shown in Figs. 6(a) and 9(a). This deterioration in the performance of the FCC technique might have been caused by introducing the additional assumption expressed in Eq. (6). When no deformation exists, the FCC technique introduces only a single and valid assumption as expressed in Eq. (6), namely that the cross-correlation coefficient depends on the value of the beam overlap area. Therefore, the FCC technique succeeded in compensating for the error involved in the

speckle tracking method almost perfectly under the condition that cross-correlation coefficients were calculated accurately. In the presence of deformation, the FCC technique introduces the assumption that the cross-correlation depends on the spatio-temporal distance given by Eq. (6). Equation (7) indicates that the FCC technique works correctly for any value of β ; however, there is no information regarding the relationship between the effect of the passage of time on the cross-correlation and the effect of the horizontal distance. Therefore, the additional assumption expressed in Eq. (6) has average validity, and the average validity of this equation might have caused the suppression of the FCC performance. However, the deformation severely reduces the estimation accuracy of the conventional speckle-tracking method, and thus the employment of the FCC is beneficial in the case of deformation, as shown in Fig. 9. Future work should take account of the beam-width variation caused by the measurement depth.

The proposed method can be applied in the case of using a transmit beam. That is, this work includes no investigation into the application to the high-frame-rate imaging method using parallel beamforming with an unfocused transmit beam.⁴³⁾ Simultaneous acquisition of the received signals of all scan lines using parallel beamforming also suppresses the effect of out-of-plane motion and deformation on lateral-velocity estimation.

5. Conclusions

In the current study, we reported on the intrinsic error involved in a speckle tracking method caused by out-of-plane motion and deformation. We proposed a compensation method for this intrinsic error that requires no a priori information, and we investigated the performance of the proposed compensation method in simulation and experimental studies. When the beam-spot interval on the tissue was half the beam-spot width or less, the RMSE of the estimated tissue motion velocity calculated using the proposed method ranged from 6.4 to 34% of that using the conventional speckle-tracking method. This study shows the high potential of the proposed compensation method for improving the estimation of tissue motion velocity using an ultrasound cross-correlation technique in medical diagnosis, such as in the assessment of cardiac function.

Acknowledgments

This work is partly supported by the Innovative Techno-Hub for Integrated Medical Bio-Imaging of the Project for Developing Innovation Systems from the Ministry of Education, Culture, Sports, Science and Technology, Japan (MEXT), and by MEXT/JSPS KAKENHI Grant Number 25870345.

- 1) G. E. Trahey, J. W. Allison, and O. T. Von Ramm, *IEEE Trans. Biomed. Eng.* **BME-34**, 965 (1987).
- 2) P. M. Embree and W. D. O'Brien, *IEEE Trans. Ultrason. Ferroelectr. Freq. Control* **37**, 176 (1990).
- 3) B. F. Osmanski, M. Pernot, G. Montaldo, A. Bel, E. Messas, and M. Tanter, *IEEE Trans. Med. Imaging* **31**, 1661 (2012).
- 4) H. Takahashi, H. Hasegawa, and H. Kanai, *Jpn. J. Appl. Phys.* **53**, 07KF08 (2014).
- 5) J. Ophir, *Ultrason. Imaging* **13**, 111 (1991).
- 6) M. O'Donnell, A. R. Skovoroda, B. M. Shapo, and S. Y. Emelianov, *IEEE Trans. Ultrason. Ferroelectr. Freq. Control* **41**, 314 (1994).
- 7) J. Kybic and M. Unser, *IEEE Trans. Image Process.* **12**, 1427 (2003).
- 8) H. Shida, H. Hasegawa, and H. Kanai, *Jpn. J. Appl. Phys.* **51**, 07GF05 (2012).
- 9) S. W. Flax and M. O'Donnell, *IEEE Trans. Ultrason. Ferroelectr. Freq. Control* **35**, 758 (1988).
- 10) G. C. Ng, S. S. Worrell, P. D. Freiburger, and G. E. Trahey, *IEEE Trans. Ultrason. Ferroelectr. Freq. Control* **41**, 631 (1994).
- 11) D. Asari, H. Hasegawa, and H. Kanai, *Jpn. J. Appl. Phys.* **53**, 07KF21 (2014).
- 12) M. Sato, H. Hasegawa, and H. Kanai, *Jpn. J. Appl. Phys.* **53**, 07KF03 (2014).
- 13) K. Kitamura, H. Hasegawa, and H. Kanai, *Jpn. J. Appl. Phys.* **51**, 07GF08 (2012).
- 14) Y. Honjo, H. Hasegawa, and H. Kanai, *Jpn. J. Appl. Phys.* **51**, 07GF06 (2012).
- 15) H. Kanai and M. Tanaka, *Jpn. J. Appl. Phys.* **50**, 07HA01 (2011).
- 16) L. Bohs and G. Trahey, *IEEE Trans. Biomed. Eng.* **38**, 280 (1991).
- 17) V. Behar, D. Adam, P. Lysyansky, and Z. Friedman, *Ultrasonics* **43**, 57 (2004).
- 18) M. Lubinski, S. Emelianov, and M. O'Donnell, *IEEE Trans. Ultrason. Ferroelectr. Freq. Control* **46**, 82 (1999).
- 19) J. Crosby, B. Amundsen, T. Hergum, E. Remme, S. Langeland, and H. Torp, *Ultrasound Med. Biol.* **35**, 458 (2009).
- 20) M. Ledesma-Carbayo, J. Kybic, M. Desco, A. Santos, M. Suhling, P. Hunziker, and M. Unser, *IEEE Trans. Med. Imaging* **24**, 1113 (2005).
- 21) B. Zitová and J. Flusser, *Image Vision Comput.* **21**, 977 (2003).
- 22) O. Goksel, H. Eskandari, and S. E. Salcudean, *IEEE Trans. Med. Imaging* **32**, 408 (2013).
- 23) O. Goksel and S. E. Salcudean, *IEEE Trans. Med. Imaging* **30**, 11 (2011).
- 24) H. Eskandari, S. E. Salcudean, R. Rohling, and J. Ohayon, *Phys. Med. Biol.* **53**, 6569 (2008).
- 25) B. Heyde, R. Jasaityte, D. Barbosa, V. Robesyn, S. Bouchez, P. Wouters, F. Maes, P. Claus, and J. D'Hooge, *IEEE Trans. Med. Imaging* **32**, 449 (2013).
- 26) R. Z. Azar, A. Baghani, S. E. Salcudean, and R. Rohling, *IEEE Trans. Ultrason. Ferroelectr. Freq. Control* **57**, 2421 (2010).
- 27) J. M. Abeyssekera, R. Zahir-Azar, O. Goksel, and R. Rohling, *Ultrasonics* **52**, 156 (2012).
- 28) L. de Isla, D. Balcones, C. Fernández-Golfín, P. Marcos-Alberca, C. Almería, J. Rodrigo, C. Macaya, and J. Zamorano, *J. Am. Soc. Echocardiogr.* **22**, 325 (2009).
- 29) P. Reant, L. Barbot, C. Touche, M. Dijos, F. Arzac, X. Pillois, M. Landelle, R. Roudaut, and S. Lafitte, *J. Am. Soc. Echocardiogr.* **25**, 68 (2012).
- 30) F. Maffessanti, H.-J. Nesser, L. Weinert, R. Steringer-Mascherbauer, J. Niel, W. Gorissen, L. Sugeng, R. M. Lang, and V. Mor-Avi, *Am. J. Cardiol.* **104**, 1755 (2009).
- 31) K. Saito, H. Okura, N. Watanabe, A. Hayashida, K. Obase, K. Imai, T. Maehama, T. Kawamoto, Y. Neishi, and K. Yoshida, *J. Am. Soc. Echocardiogr.* **22**, 1025 (2009).
- 32) R. Jasaityte, B. Heyde, V. Ferferieva, B. Amundsen, D. Barbosa, D. Loeckx, G. Kiss, F. Orderud, P. Claus, H. Torp, and J. D'hooge, *Int. J. Cardiol. Imaging* **28**, 1049 (2012).
- 33) M. De Craene, S. Marchesseau, B. Heyde, H. Gao, M. Alessandrini, O. Bernard, G. Piella, A. R. Porras, L. Tautz, A. Hennemuth, A. Prakosa, H. Liebgott, O. Somphone, P. Allain, S. Makram Ebeid, H. Delingette, M. Sermesant, J. D'hooge, and E. Saloux, *IEEE Trans. Med. Imaging* **32**, 1632 (2013).
- 34) H. Taki, T. Sakamoto, M. Yamakawa, T. Shiina, and T. Sato, *Proc. IEEE Ultrasonics Symp.*, 2012, p. 2563.
- 35) B. H. Briggs, *Handbook for MAP* (ICSU, Paris, 1984) Vol. 13, p. 166.
- 36) M. Yamamoto, T. Sato, T. Tsuda, S. Fukao, and S. Kato, *Pure Appl. Geophys.* **130**, 605 (1989).
- 37) D. A. Holdsworth and I. M. Reid, *Ann. Geophys.* **22**, 3829 (2004).
- 38) F. Viola and W. F. Walker, *IEEE Trans. Ultrason. Ferroelectr. Freq. Control* **50**, 392 (2003).
- 39) J. Luo and E. E. Konofagou, *IEEE Trans. Ultrason. Ferroelectr. Freq. Control* **57**, 1347 (2010).
- 40) J. Udesen, F. Gran, K. L. Hansen, J. A. Jensen, C. Thomsen, and M. B. Nielsen, *IEEE Trans. Ultrason. Ferroelectr. Freq. Control* **55**, 1729 (2008).
- 41) R. Zahir-Azar and S. E. Salcudean, *IEEE Trans. Biomed. Eng.* **53**, 1990 (2006).
- 42) H. Taki, K. Taki, T. Sakamoto, M. Yamakawa, T. Shiina, M. Kudo, and T. Sato, *IEEE Trans. Med. Imaging* **31**, 417 (2012).
- 43) H. Hasegawa and H. Kanai, *Jpn. J. Appl. Phys.* **53**, 07KF02 (2014).